Investigation of the Relationship between Dipolar Properties and Cis−Trans Configuration in Retinal Polyenes: A Comparative Study Using Stark Spectroscopy and Semiempirical Calculations

Sarah A. Locknar and Linda A. Peteanu*

Department of Chemistry, Carnegie Mellon University, Pittsburgh, Pennsylvania 15213

Received: December 18, 1997; In Final Form: March 11, 1998

Three biologically active conformers of retinal, all-trans, 9- and 13-cis, and their Schiff bases (SB), are studied using a combination of electroabsorption (Stark) spectroscopy and semiempirical calculations. All of the retinal isomers studied show both a large change in dipole moment between the ground and excited states ($|\Delta\underline{\mu}|$ greater than 8 D) and a large change in polarizability between the ground and excited states ($\overline{\Delta\alpha}$ greater than 300 Å^3). The experimental $|\Delta\underline{\mu}|$ values in the aldehydes are well predicted by semiempirical calculations. However, the calculated $\Delta\mu$ values for the SB are more than 2 times smaller than experimental values. This discrepancy suggests mixing of the $1B_u$ state with another state with a large dipole moment, most likely the $2A_g$ state, which is not probed by our calculational method. For both the aldehydes and SB, $\overline{\Delta\alpha_{calc}}$ values are 2−8 times lower than experimental values. Possible reasons for the deviation between theory and experiment are discussed.

Introduction

Retinal is a common photopigment in nature (Figure 1) that has several biologically active cis-double-bond conformers. In rhodopsin, it is found in the 11-cis or 9-cis forms, which isomerize to all-trans,[1] and in bacteriorhodopsin, the all-trans form isomerizes to the 13-cis configuration.[2] In these systems, the absorption of a photon by retinal induces a photoisomerization that subsequently drives a conformational change in the protein.[3−5] In addition to their important biological role, retinals and retinal proteins also exhibit large hyperpolarizabilities, which have made them attractive for nonlinear optical applications.[6]

In order to model the isomerization process, absorption profiles, and nonlinear optical properties of these molecules, numerous groups have sought to calculate the low-lying electronic levels of retinal.[6−11] Conventionally, the energy levels in retinals are described using the C_{2h} symmetry labels even though these are recognized to be approximate. The ground state has A_g symmetry and the closest lying singlet excited states are the $1B_u$ and the $2A_g$ states. The $1B_u$ state is directly accessible from the ground state by a one-photon absorption, while the $2A_g \leftarrow 1A_g$ transition is one-photon forbidden in linear polyenes. Based on two-photon spectroscopy[12,13] and calculations,[7] the $2A_g$ state in both retinals and their Schiff bases is observed to lie below the $1B_u$ state in energy and is thought to be populated by a nonradiative crossing, which then leads to isomerization.[14−16]

One of the current goals of this area of research is to gain information about the electronic energy levels and isomerization pathways of retinals and how these depend on conformation and environment. It is known, for example, that the relative energies of the interactions between excited states differ between isomers and as a function of temperature and solvent polarity.[17−20] Also, the quantum yields of photoisomerization increase with solvent polarity[18,20] and depend on double-bond conformation. The protein exploits these polarity-dependent properties to tune the wavelength of absorption of the protonated Schiff base (SB) chromophore[21] and its photoreactivity.

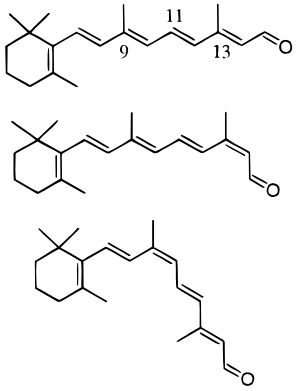

Figure 1. Structure and numbering of retinals: top, ATR; middle, 13-CR; bottom, 9-CR. In the Schiff base forms of the retinals, the oxygen is replaced with an *n*-butylamine group.

To better understand the effect of the environment on retinal properties, it is desirable to have a quantitative measure of the changes in dipole moment and polarizability that occur following photon absorption. Such information can be obtained directly by using Stark effect (electroabsorption) spectroscopy. This technique measures the perturbation to the absorption spectrum as a result of applying an electric field. The results of this measurement provide a good test of gas-phase semiempirical calculations and how the properties of the molecule change with solvation. This paper is a systematic study, using electroabsorption data and semiempirical calculations, of the three most stable forms of retinal and their SB forms in order to begin to understand the roles that solvation and double-bond conformation play in their photophysical behavior. While we obtain good agreement between calculated and measured dipole moments, our results show that the excited-state polarizabilities of these molecules increase dramatically in the condensed phase, beyond what can be predicted using a simple reaction field theory.[22]

S1089-5647(98)00562-8 CCC: $15.00
Published on Web 04/30/1998

Experimental Section

Electroabsorption Spectrometer. A schematic of the electroabsorption spectrometer can be found in Figure 2. The light from a 150W Xe arc lamp (Oriel 66057) is directed through a 0.3 m pathlength monochromator (Spex 340S), a depolarizer, and Glan-Taylor prism (Karl Lambrect, Chicago, IL) to select horizontal polarization. Lenses focus the beam onto the sample and then onto the detector. The detector is a UV-sensitized photodiode with an internal op-amp (UDT Sensors, Inc. Hawthorne, CA, UDT-020UV) powered by a dc power supply (BK 1651) which is continually adjustable between zero and 20 V dc. An electric field of approximately 10^6 V/cm and 450 Hz is applied to the sample through optically transparent electrodes of indium tin oxide (ITO) coated glass. The ac power supply used (Joseph Rolphe Assoc. Palo Alto, CA, model 1100) is continuously adjustable in frequency from zero to 460 Hz and in voltage from 200 V to 15 kV peak to peak. The ac field induces a modulation of transmission intensity which is approximately 1 part in 10^6 of the total light intensity. A lock-in amplifier (Stanford Research Systems, SR850), triggered by the frequency reference channel of the high-voltage power supply, simultaneously detects the second harmonic of the applied ac field frequency and the total intensity of the sample (unmodulated). The lock-in amplifier and monochromator are driven with a Dell Dimension computer with an interface written with the Lab Windows package (National Instruments).

Sample Preparation. The molecule of interest and poly(methyl methacrylate) (PMMA) were dissolved together in dichloroethane at a concentration of about 75 μmol retinal/g PMMA. The solution was gravity filtered into an aluminum dish containing ITO-coated glass slides (250 Å thick, Kargo Ltd. Inc. Akron, OH). After evaporation onto the glass at room temperature, another piece of ITO-coated glass was glued with a thick PMMA solution onto the PMMA-coated glass to create a "sandwich", which was clamped together and put in the refrigerator to set overnight to reduce the possibility of thermal isomerization products. This method produced "glass-like" films in the thickness range 20−80 μm. To get a more accurate measure of the film thickness, an interference pattern of fringes was measured in the 900−2500 nm range using a UV−vis−NIR absorption spectrometer (Perkin Elmer Lambda 900). The spacing between adjacent peaks or valleys (λ_1 and λ_2) in the fringe pattern is related to the thickness by the following: thickness $= \lambda_1\lambda_2/(2n(\lambda_1 - \lambda_2))$, where n is the refractive index (1.49 for PMMA). This interference method gave a standard deviation in the thickness of 1.5−10 μm depending on the uniformity of the polymer film. Since this was the major source of error in our measurements, an average weighted by the standard deviation of the thickness was used to determine the electric field parameters and the standard deviation in these parameters.[23]

Materials. All-trans (ATR), 9-cis (9-CR), and 13-cis (13-CR) retinals (Aldrich) were used without further purification. The purity of ATR was above 90% as determined by integrating the ^{1}H NMR peaks associated with the proton on carbon 15, and the purity of the cis isomers reported by Aldrich was also above 90%. In all cases, other isomers are the main impurities.[24] All samples were prepared and handled under dim red light. Poly(methyl methacrylate) (Aldrich) and dichloroethane were used without further purification. *N*-Butylamine Schiff bases of the retinals of interest were prepared by the method of Irving and Leermakers.[25] After the reaction was completed, the samples were evaporated and frozen for later use or immediately dissolved in dichloroethane for film casting.

Theory of Electroabsorption. The theory behind electroabsorption was developed by Liptay[26] and is summarized here with some slight changes in formalism. The overall change in transmitted light intensity caused by the application of an electric field is described by the following equation:

$$\left(\frac{2\sqrt{2}}{2.303}\right)\frac{\Delta I}{I} = \underline{\epsilon}^2\left[a_\chi A(\nu) + b_\chi \frac{\partial A(\nu)}{\partial \nu} + c_\chi \frac{\partial^2 A(\nu)}{\partial \nu^2}\right]$$

The $\Delta I/I$ term is a measure of the intensity change as a result of the applied field normalized to the total light intensity reaching the detector. They were measured simultaneously by the lock-in amplifier, using both the locked (ΔI) and total voltage (I) channels. The factor of $2\sqrt{2}$ is needed to convert from rms voltage (read in by the lock-in amplifier) to an equivalent dc voltage, and the factor of 2.303 is derived from treating the field-induced intensity change as a perturbation to the intensity. The $A(\nu)$ represents the absorption as a function of frequency, and $\underline{\epsilon}$ represents the applied field in V/cm. In several experiments involving the measurements of electric field effects on retinals in the literature,[27−29] an internal field factor was included in the field term (i.e., $\underline{\epsilon} = f(\underline{\epsilon}_{\text{applied}})$. However, as it is experimentally very difficult to determine the internal field, our reported values for $|\underline{\mathbf{m}}\cdot\Delta\underline{\mu}|$, $|\Delta\underline{\mu}|$, $\Delta\underline{\underline{\alpha}}_{\text{m}}$, and $\overline{\Delta\alpha}$ will not include this correction and will thus be about 20% larger than if the correction had been included. For comparison, the internal field factor (f) for PMMA has been estimated to be 1.111.[27]

The constants a_χ, b_χ, and c_χ are defined as follows.[26]

$$a_\chi = \frac{1}{30|\underline{\mathbf{m}}|^2}\sum_{i,j}[10A_{ij}^2 + (3A_{ii}A_{jj} + 3A_{ij}A_{ji} - 2A_{ij}^2)(3\cos^2\chi - 1)] + \frac{1}{15|\underline{\mathbf{m}}|^2}\sum_{i,j}[10\mathbf{m}_i B_{ijj} + (3\mathbf{m}_i B_{jij} - 3\mathbf{m}_i B_{jji} - 2\mathbf{m}_i B_{ijj})(3\cos^2\chi - 1)] + \frac{\beta}{15|\underline{\mathbf{m}}|^2}\sum_{i,j}[10\mathbf{m}_i A_{ij}\mu_{gj} + (3\mathbf{m}_i A_{ji}\mu_{gj} + 3\mathbf{m}_i A_{jj}\mu_{gi} - 2\mathbf{m}_i A_{ij}\mu_{gj})(3\cos^2\chi - 1)] + \frac{\beta}{10}(\alpha_{gm} - \overline{\alpha}_g)(3\cos^2\chi - 1) + \frac{\beta^2}{30}[3(\hat{\mathbf{m}}\cdot\underline{\Delta\mu})^2 - |\underline{\mu}_g|^2](3\cos^2\chi - 1) \quad (1)$$

$$b_\chi = \frac{1}{15|\underline{\mathbf{m}}|^2}\sum_{i,j}[\mathbf{m}_i A_{ij}\Delta\mu_j + (3\mathbf{m}_i A_{ji}\Delta\mu_j + 3\mathbf{m}_i A_{jj}\Delta\mu_i - 2\mathbf{m}_i A_{ij}\Delta\mu_j)(3\cos^2\chi - 1)] + \frac{1}{2}\overline{\Delta\alpha} + \frac{1}{10}[\Delta\underline{\underline{\alpha}}_{\text{m}} - \overline{\Delta\alpha}](3\cos^2\chi - 1) + \frac{\beta}{3}(\underline{\mu}_g\cdot\underline{\Delta\mu}) + \frac{\beta}{15}[3(\hat{\mathbf{m}}\cdot\underline{\mu}_g)(\hat{\mathbf{m}}\cdot\underline{\Delta\mu}) - (\underline{\mu}_g\cdot\underline{\Delta\mu})](3\cos^2\chi - 1) \quad (2)$$

$$c_\chi = \frac{1}{6}|\Delta\underline{\mu}|^2 + \frac{1}{30}[3(\hat{\mathbf{m}}\cdot\Delta\underline{\mu})^2 - |\Delta\underline{\mu}|^2](3\cos^2\chi - 1) \quad (3)$$

The symbols α and μ represent the polarizability and dipole moment, respectively. The Δ signifies the change between the ground-state (subscript g) and excited-state properties of the molecule. The transition moment is represented by $\underline{\mathbf{m}}$ ($\hat{\mathbf{m}}$ is a unit vector along the transition moment axis), and a subscript m indicates a component of the parameter along the transition

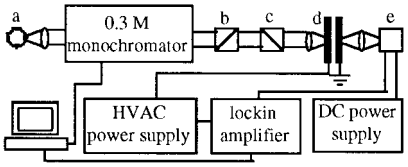

Figure 2. Structural diagram of electroabsorption instrument. The light source (a), depolarizer (b), polarizer (c), sample (d), and photodiode detector (e) and other components are described in detail in the text.

moment axis (i.e., $\Delta\underline{\underline{\alpha}}_m = \hat{\mathbf{m}}\cdot\Delta\underline{\underline{\alpha}}\cdot\hat{\mathbf{m}}$). The tensors $\underline{A}$ and $\underline{\underline{B}}$ represent the transition polarizability and hyperpolarizability, respectively, as a result of the effect of the applied electric field on the molecular transition moment: $\underline{\mathbf{m}}(\epsilon) = \underline{\mathbf{m}} + \underline{A}\cdot\underline{\epsilon} + \underline{\epsilon}\cdot\underline{\underline{B}}\cdot\underline{\epsilon}$. Because the $\underline{A}$ and $\underline{\underline{B}}$ terms are usually thought to be small, we set them to zero when calculating our changes in dipole moment and polarizability. However, inclusion of the a_χ term is essential for a good fit to the electroabsorption spectrum. In our polymer samples, we also assume that the molecules are isotropic and fixed in orientation, so during our analysis, all factors containing the Boltzmann factor (β) are neglected. These two approximations will be addressed in a later section. A bar indicates the average (i.e., $\overline{\Delta\alpha} = (1/3)\mathrm{Tr}(\Delta\underline{\underline{\alpha}})$) and χ represents the angle between the applied electric field and the electric field vector of the light. The indices i and j label the vector/tensor components along x, y, and z.

The above terms can also be described qualitatively to get a physical understanding of electric field effects on molecules. The a_χ term describes the field-induced changes in the transition moment. It is manifested as an overall change in intensity of the absorption profile. The a_χ expression contains many terms which depend on the Boltzmann factor (eq 1), which make it sensitive to molecular alignment in the field. The b_χ term depends mainly on the interaction of the molecular polarizability with the applied field. Because the excited-state polarizability in polyenes is larger than in the ground state, the electric field serves to shift the absorption spectrum to longer wavelengths. The difference between the shifted and unshifted spectra ($\Delta I/I$) can be described as the first derivative of the unperturbed absorption spectrum. The c_χ term describes the interaction of the molecular dipole moment with the applied field. Because our system is isotropic, this causes a broadening of the absorption spectrum (an equal number of molecules are aligned parallel and antiparallel to the applied field). The difference between the broadened spectrum and the unperturbed spectrum results in a shape like the second derivative of the unperturbed absorption spectrum.

The electroabsorption spectrum is fit to the unperturbed absorption spectrum and its first and second numerical derivatives simultaneously using a least-squares fitting routine written with Matlab (the Mathworks). In cases where the optical density of the sample was low, or the noise level was particularly high, the absorption spectrum was first fit to one or two Gaussians using a simplex method (EZfit[30]).

Semiempirical Calculations. Ground-state geometries were optimized using the AM1[31] molecular orbital procedure (Mopac). Ground- and excited-state dipole moments were calculated using expectation values generated from both MNDO/SCI[32−34] (Hyperchem) and INDO1S/SCI (Argus). Polarizabilities were obtained with a finite-field method[35,36] using the dipole expansion of perturbed INDO1S/SCI[37,38] molecular orbitals. Reaction field corrections to the calculated values were performed using the following expressions to obtain "solvated" estimates for the dipolar properties:[22]

$$\Delta\mu = \frac{1 - f'\overline{\alpha_g}}{(1 - f'\overline{\alpha_e})(1 - f\overline{\alpha_g})}\left[\mu_e - \frac{\mu_g(1 - f\overline{\alpha_e})}{1 - f\overline{\alpha_g}}\right] \quad (4)$$

$$\overline{\Delta\alpha} = \frac{1}{(1 - f'\overline{\alpha_e})(1 - f\overline{\alpha_g})}\left[\overline{\alpha_e} - \overline{\alpha_g} + (f - f')\overline{\alpha_g}\left(\overline{\alpha_e} - \frac{\overline{\alpha_g}(1 - f\overline{\alpha_e})}{(1 - f\overline{\alpha_g})}\right)\right] \quad (5)$$

where

$$f = \frac{3}{a^2 b}\left(\frac{A(1 - A)(\epsilon - 1)}{\epsilon + A(1 - \epsilon)}\right) \quad \text{and}$$

$$f' = \frac{3}{a^2 b}\left(\frac{A(1 - A)(n^2 - 1)}{n^2 + A(1 - n^2)}\right)$$

Here α represents the calculated polarizability in the gas phase of the ground or excited state, μ represents the dipole moment in the gas phase of the ground or excited state, a is the short axis of the ellipsoidal cavity, and b is the long axis of the ellipsoidal cavity (both estimated from AM1 optimized geometries). A is related to the ellipticity of the cavity and is estimated from the ratio of b/a as described by Bottcher.[39] The dielectric constant (ϵ) for PMMA is 3.9,[40] and n is the refractive index for PMMA (1.49). Because of the polar and polarizable nature of the retinals, these solvation corrections are significant and cannot be neglected.

Results

Figure 3 shows the electroabsorption of 13-CR and the components of the derivatives used to fit the spectrum. Note that the first derivative dominates the fitting, illustrating a large change in polarizability upon photon absorption. The electroabsorption spectra of the 9-cis isomer of retinal with its Schiff base at both $\chi = 55°$ and 90° together with their calculated fits are shown in Figure 4. These spectra are adequately described by one set of electric field parameters (a_χ, b_χ, c_χ) as seen by the high quality of the fits to the data. This suggests that only one electronic transition is being probed. Samples run at liquid nitrogen temperatures gave results that were within 20% of room-temperature values, suggesting that the extent of field-induced molecular alignment in the PMMA films should be minimal. Furthermore, the value of a_χ we obtain in the ATR/PMMA film (Table 1) is similar to that measured in a frozen 3-methylpentane glass (not shown) and to a_χ values reported for other donor−acceptor polyenes in frozen glasses.[41,42] The dipolar properties of the retinal isomers together with the results obtained with calculations are summarized in Table 1.[43] As expected, the difference between $|\Delta\underline{\mu}|$ and $|\underline{\mathbf{m}}\cdot\Delta\underline{\mu}|$ is larger in the cis isomers due to the increased angle between the transition moment and $|\Delta\underline{\mu}|$.

If the change in polarizability between the ground and excited state lies mostly along the transition moment, $\overline{\Delta\alpha}$ would be 1/3 of $\Delta\underline{\underline{\alpha}}_m$. This is roughly what we observe in the aldehyde series (Table 1). In contrast, the SB isomers exhibit $\Delta\underline{\underline{\alpha}}_m/\overline{\Delta\alpha}$ ratios that range from greater than 5 in ATR-SB to less than 3 for 9-CR-SB (Table 1). To get a value of $\Delta\underline{\underline{\alpha}}_m/\overline{\Delta\alpha}$ greater (less) than 3, a significant decrease (increase) in polarizability between the excited and ground states must occur along axes orthogonal to the transition moment. Therefore, components orthogonal to the transition moment axis contribute

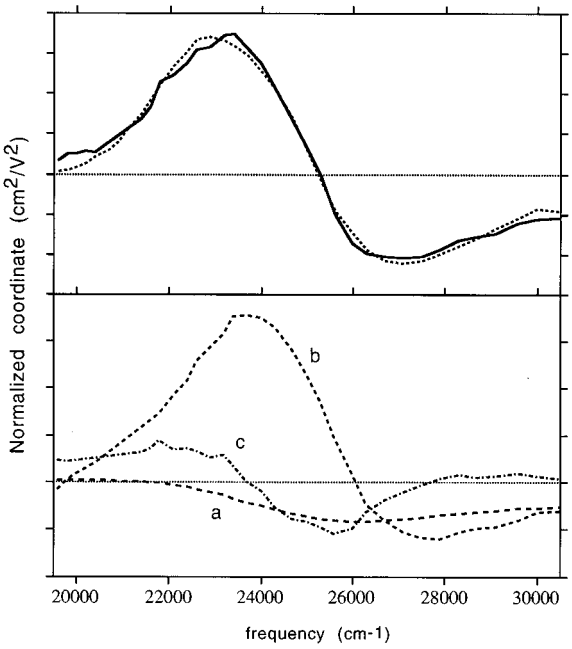

Figure 3. Top: Electroabsorption spectra (solid line) and fit (dashed line) of 13-CR at $\chi = 55°$ in PMMA film. Bottom: Zeroth (a), first (b), and second (c) derivative contributions to the overall electroabsorption fit. The *y*-axis "normalized coordinate" is the result of dividing $\Delta I/I$ by $\bar{\epsilon}^2$ in the process of fitting the data to the absorption spectrum and its derivatives.

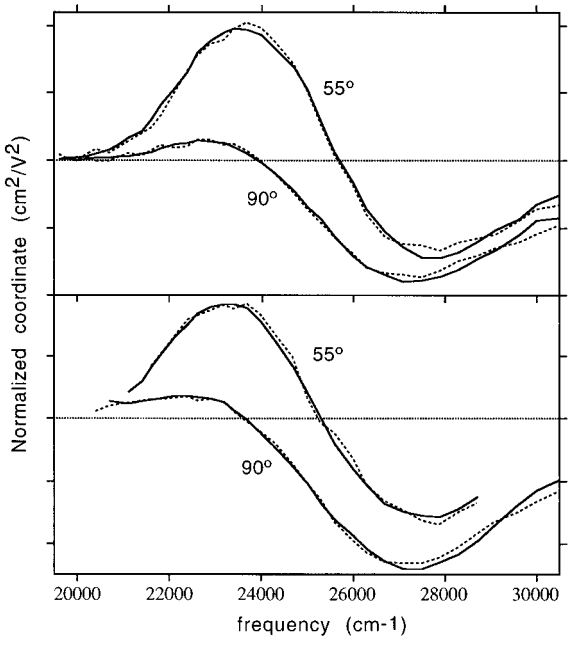

Figure 4. Electroabsorption spectra of 9-CR (top) and 9-CR-SB (bottom) in PMMA film. Data are shown with the solid line, and the fit to absorption is shown with the dashed line. The two angles shown correspond to χ (see theory section).

more to $\overline{\Delta\alpha}$ in the SB forms of retinal. This is also observed in our calculations (not shown). A striking result is the large magnitude of both $\overline{\Delta\alpha}$ and $\Delta\underline{\underline{\alpha}}_m$ within the PMMA matrix. The remainder of this paper will attempt to predict these measured quantities using semiempirical calculations.

Comparison of Experimental and Calculated Values. We shall begin with a look at the accuracy of the calculated ground-state properties of the retinals. The AM1 geometry optimization routine gave results very close to the published X-ray crystallographic data[44−46] (less than 5% deviation in bond lengths, angles, and torsions), except for two single bond rotations. The torsions about both the C_8-C_9 and C_6-C_7 bonds are rotated through the plane of the polyene chain with respect to the crystal structure (up to 20° and 120°, respectively). Despite this discrepancy, $\overline{\Delta\alpha}_{calc}$ and $\Delta\mu_{calc}$ values for AM1 and crystal geometries were within 20% of each other (not shown).

The calculated ground state and changes in dipole moment upon photon absorption in the gas phase are summarized in Table 2. The calculations of μ_g using MNDO are within about 20% of both ab initio and values obtained by experiment in both ATR and ATR-SB (Table 2). The μ_g calculated for ATR using INDO/SCI are larger than measured and calculated values, but inclusion of configuration interaction at the doubles level (SDCI) tends to lower the ground-state dipole moment to within an acceptable error.[47] These results indicate that inclusion of SDCI is necessary for accurate μ_g values using INDO, but not for MNDO.

Changing our focus to calculated values of $\Delta\mu$, we realize that it is difficult to ascertain which method is more accurate, because arguments can be made for both. In the case of the MNDO/SCI calculation, it can be argued that since this method more accurately predicts μ_g in ATR, it should be the better method for calculating $\Delta\mu$. However, one could also argue that the INDO/SCI method is more reliable because it is parametrized for spectroscopy and difference values (i.e., energy differences and perhaps difference dipole moments). It should also be noted that the solvent correction applied to $\Delta\mu_{calc}$ is highly sensitive to both ground- and excited-state polarizabilities (vide infra). We observe excellent agreement between the finite-field and sum-over-states methods in the literature (Table 2). Addition of solvent corrections in the aldehydes bring $\Delta\mu_{INDO}$ values within 10−25% of our measured results (Table 1), while $\Delta\mu_{MNDO}$ values remain a factor of 2 smaller than experimental values.

In the SB series, the agreement between calculated and measured $\Delta\mu$ values is much worse for both semiempirical methods. The $\Delta\mu_{INDO}$ values are roughly 2 times smaller and $\Delta\mu_{MNDO}$ values are 3−5 times smaller than measured values (Table 1). This discrepancy may be due to mixing between the 1^1B_u and 2^1A_g states. The all-trans form has the largest oscillator strength for the $1B_u \leftarrow 1A_g$ transition (Table 3). As one would expect, as the polyene loses C_{2h} symmetry by displacement of the cis double bond toward the middle of the chain, the contribution of other "unallowed" states increases. The two-photon absorption spectrum of ATR-SB[13] reveals a much broader $2A_g \leftarrow 1A_g$ band than that observed in ATR,[12] which may indicate mixing between the $1B_u$ and $2A_g$ states. The $2A_g$ state is also predicted to have a larger dipole moment than the $1B_u$ state in ATR[12] and some other conformers,[47] which could lead to a larger experimental $|\Delta\underline{\mu}|$ if significant mixing occurs in the excited state or if the oscillator strength of the $2A_g \leftarrow 1A_g$ transition depends on cis bond location. As the $1B_u \leftarrow 1A_g$ oscillator strength is smaller in the cis isomers than ATR-SB (Table 3), it is reasonable to expect that the $2A_g \leftarrow 1A_g$ oscillator strength would be larger in the cis isomers.

We now turn our attention to the polarizability calculations. The gas-phase α_g (INDO) of ATR along the principal moment of inertia ($\alpha_{zz} = 62$ Å^3) is within about 30% of both gas-phase ab initio[11] ($\alpha_{zz} = 41$ Å^3) and values obtained from refractive index measurements[27] ($\alpha_{zz} = 78$ Å^3). Calculated gas-phase $\overline{\alpha_g}$ for ATR-SB were slightly higher than gas-phase ab initio $\overline{\alpha_g}$ values reported in the literature (35 vs around 26 Å^3).[10] However, the ab initio results did not include the *n*-butyl group in their calculations and would be expected to be slightly smaller

TABLE 1: Changes between Ground- and Excited-State Properties of Retinals in PMMA Films[a]

	$f\|\mathbf{m}\cdot\Delta\underline{\mu}\|$	$f\|\Delta\underline{\mu}\|$	$\Delta\mu_{INDO}$	$\Delta\mu_{MNDO}$	$f^2\Delta\underline{\alpha}_m$	$f^2\overline{\Delta\alpha}$	$\overline{\Delta\alpha_{calc}}$	$a_\chi \times 10^{15}$
ATR	12.3 ± 0.4	12.2 ± 0.4	13.5 ± 0.7	6.6 ± 0.3	1034 ± 73	311 ± 22	57 ± 3	−2.4 ± 0.2
13-CR	7.2 ± 0.5	10.3 ± 0.6	12.9 ± 0.7	6.0 ± 0.3	1651 ± 196	444 ± 53	54 ± 3	−1.7 ± 0.2
9-CR	9.5 ± 0.4	11.6 ± 0.5	12.6 ± 0.6	5.7 ± 0.4	1582 ± 138	425 ± 37	56 ± 3	−3.4 ± 0.6
ATR-SB	8.9 ± 0.4	8.5 ± 0.4	5.4 ± 0.2	2.2 ± 0.1	821 ± 70	157 ± 14	86 ± 5	−1.1 ± 0.1
13-CR-SB	13.7 ± 0.4	13.4 ± 0.4	5.8 ± 0.2	2.7 ± 0.1	868 ± 57	252 ± 17	80 ± 5	−1.5 ± 0.1
9-CR-SB	10.9 ± 1.2	13.3 ± 1.4	5.5 ± 0.2	2.6 ± 0.1	587 ± 154	229 ± 54	84 ± 5	−2.2 ± 0.5

[a] Polarizabilities are reported in Å^3 and represent the average over all directions, dipole moments are reported in debye (D), and a_χ values are reported in cm^2/V^2. All experimental values are the result of a weighted average (see Experimental Section) of four or more duplicate samples. $\Delta\mu_{INDO}$, $\Delta\mu_{MNDO}$, and $\overline{\Delta\alpha_{calc}}$ are the results of applying the solvation correction to calculated values in Table 3 (see Experimental Section), and the errors in these values arise from a 10% estimated error in the solvent cavity volume. An estimate for the internal field factor (f) for PMMA is 1.111 (see ref 27).

TABLE 2: Calculated Gas-Phase Properties of Retinals[a]

	this work						literature	
	INDO/SCI/FF				MNDO/SCI			
	$\overline{\alpha_g}$	$\overline{\Delta\alpha}$	μ_g	$\Delta\mu$	μ_g	$\Delta\mu$	$\Delta\mu^b$	μ_g
ATR	31	40	8.4	9.2	3.8	4.6	8.9	4.8[c], 3.2[d] 3.2[e], 4.9[f]
13-CR	30	36	8.3	8.5	3.9	4.0	8.5	
9-CR	29	39	8.5	8.4	3.9	3.8	8.3	
ATR-SB	35	69	4.1	4.0	1.6	1.7	5.7	1.25[e]
13-CR-SB	34	64	4.3	4.4	1.8	2.1	4.7	
9-CR-SB	34	66	4.6	4.0	1.8	1.9	5.1	

[a] Polarizabilities are reported in Å^3 and are the average over all directions, and dipole moments are reported in debyes. [b] Calculated using INDO/SCI/SOS (see ref 6). [c] Calculated using INDO/SDCI (see ref 47). [d] Calculated with ab initio methods (see ref 9). [e] Measured by electroabsorption in dioxane solutions (see ref 28). These have been corrected to gas-phase values using a reaction field model.[39] [f] Measured in hexane and cyclohexane solutions using dielectric constant and refractive index data (see ref 59). It has been corrected to gas-phase values using a reaction field model.[39]

TABLE 3: Oscillator Strengths and Frequencies for the $1B_u \leftarrow 1A_g$ Transition

	INDO1S/SCI (this work)		INDO/SDCI[a]		expt[b]	
	osc. str.	ν^{-1} (cm^{-1})	osc. str.	ν^{-1} (cm^{-1})	osc. str.	ν^{-1} (cm^{-1})
ATR	1.77	28 390	1.099	28 480	1.14	25 970
13-CR	1.47	28 710	0.97	28 570	1.01	26 320
9-CR	1.43	29 000	0.92	28 470	0.97	26 350
ATR-SB	1.91	29 640			1.13	27 470
13-CR-SB	1.75	29 770			0.92	27 660
9-CR-SB	1.77	29 510			1.05	27 430

[a] See ref 8. [b] From samples in 3-methylpentane glasses at 77 K.[58]

based on this omission. Indeed, without the *n*-butyl group our $\overline{\alpha_g}$ was calculated to be 32 Å^3. A larger $\overline{\alpha_g}$ in the Schiff bases compared to the aldehyde has also been reported in other calculations.[11]

Application of the solvent corrections does not significantly improve the agreement of calculated and measured $\overline{\Delta\alpha}$ values. In the aldehydes, $\overline{\Delta\alpha_{calc}}$ remains over 5 times too small, and while the agreement is better in the SB isomers, $\overline{\Delta\alpha_{calc}}$ values are still over 1.5 times too small. To specifically evaluate the INDO1S/SCI finite-field method of excited-state polarizability calculations, we examined a series of diphenylpolyenes that share many electronic properties with retinal (Table 4). Our $\overline{\Delta\alpha_{calc}}$ for diphenylpolyenes with three double bonds or more were within about 20% of measured values. These data show that the finite-field method is useful in predicting both ground- and excited-state polarizabilities in both gas and condensed phases for nonpolar molecules like diphenylpolyenes. It remains to be understood why the polarizabilities are well modeled by the semiempirical method in a nonpolar molecule and not in a polar molecule like ATR. There are three possibilities[48] for the observed discrepancy: (1) the INDO/SCI calculation does not include enough states to correctly describe α_e in retinals, (2) the approximation used in our data analysis, that the transition moment polarizability term $\underline{A}$ (see eq 2) is negligible, is not valid, and (3) molecular orientation effects play a role in the analysis of $\overline{\Delta\alpha}$, even in frozen glasses. We shall treat these possibilities independently in the next section.

Discussion

An accurate polarizability calculation depends directly on the transition moments and inversely on the energy differences between the state of interest and other surrounding states. Calculated oscillator strengths and energies of the main one-photon absorption of retinal compared to previous calculations and to experiment are shown in Table 3. Typically, the $1B_u \leftarrow 1A_g$ transition energy decreases by about 2000 cm^{-1} upon solvation in retinals,[49] which would bring these energies close to experimental values. Our calculated oscillator strengths are about 50% too large on average, but follow the same decreasing trend across the series as the literature values (Table 3). It appears that inclusion of SDCI brings the oscillator strengths closer to measured values, as expected with greater correlation of the ground state. Overestimation of the $1B_u \leftarrow 1A_g$ oscillator strength would cause a reduction of α_e because it enhances the negative contribution to the polarizability of the $1B_u$ state.[50] However, this and higher lying states also contribute to the calculation of α_g. The good agreement between calculated α_g and literature values indicates that the overestimation of energy gaps and oscillator strengths is not a major source of error.

Semiempirical methods that use SCI are optimized to reproduce one-photon-allowed transitions from the ground state. Some of the transitions between higher lying states (such as between the $1B_u$ and other unidentified states) may be underrepresented and could be one reason for the discrepancy between measured and calculated $\Delta\alpha$ values. In an effort to identify states that may be underrepresented in these SCI calculations, we compared our calculated energies and oscillator strengths to those reported in SDCI calculations in the literature.[8] We identified several "missing" singlet $\pi^* \leftarrow \pi$ states with energies larger than the $1B_u$ state, including those with both A_g and B_u symmetry. Singlet and triplet $\pi^* \leftarrow$ n states and a triplet $\pi^* \leftarrow \pi$ state are also present in the retinals,[9] but probably do not affect the calculated polarizability of the $1B_u$ state because of the small transition moments between them. Because transitions between states with the same symmetry (i.e., B_u) are unallowed, we shall focus on those with A_g symmetry.

The effect of neglecting the $2A_g$ state on $\overline{\Delta\alpha_{calc}}$ can be predicted by locating its energy relative to the $1B_u$ state. The energy of the $2A_g$ state lies below the $1B_u$ state in most polyenes,

TABLE 4: Polarizability Calculations on Diphenylpolyenes[a]

	α_g(gas)		α_g(dioxane)		$\overline{\Delta\alpha_{calc}}$(gas)		$\overline{\Delta\alpha_{calc}}$(dioxane)	
	INDO1S	literature	INDO1S	literature	INDO1S	literature	INDO1S	literature
DPH	33		36	50[c]	69	42[c]	105	91[c]
DPO	40	49[b]	44	56[c]	86	80[b]	132	126[b]
						57[c]		116[c]
DPD	45		49	67[c]	94	70[c]	140	140[c]

[a] DPH, DPO, and DPD are diphenylhexatriene, -octatetraene, and -decapentaene, respectively. All polarizabilities are reported in Å^3 and are the average over all directions. [b] From electroabsorption measurements in cyclohexane solutions[59] (corrected to dioxane). [c] From electroabsorption measurements in dioxane solutions.[27]

so its contribution to $\overline{\alpha_e}$ would be negative. Neglecting the $2A_g$ state would thus cause $\overline{\Delta\alpha_{calc}}$ to be larger than expected. Conversely, one would expect an *increase* in $\overline{\alpha_e}$ if there is another higher energy state or states with a large oscillator strength to the $1B_u$ state. Because $\Delta\alpha_{calc}$ is *smaller* than experimental values in retinals, it appears that higher lying states are much more important than the $2A_g$ state to the calculation of $\overline{\alpha_e}$. In order to better account for the higher states, we are currently performing calculations using a semiempirical method based on SDCI.

One state that may contribute to the calculation of $\overline{\alpha_e}$ is what has been termed the mA_g state in the conjugated polymer literature.[51−54] The assignment of the integer "*m*" depends on the system. Typically, the state of A_g symmetry which both lies above the $1B_u$ state in energy and has a large two-photon oscillator strength is termed the mA_g state by convention. This state has been identified in polydiacetylenes[51,52] and β-carotene[53,54] but not yet in the retinals. In the polydiacetylenes, the transition dipole between the $1B_u$ and mA_g states is at least as large as that between the ground state and $1B_u$,[52] and in β-carotene it is about twice as large.[53,54] The energy gap between the $1B_u$ and mA_g states decreases as the length of the polydiacetylene polymer increases, theoretically reaching zero at infinite length.[55]

The mA_g state in retinals cannot be identified experimentally without additional two-photon absorption spectroscopic data, so higher lying one-photon "invisible" A_g states will be referred to in quotes. Calculations on anhydrovitamin A, a retinal analog containing no heteroatoms, identify an A_g state lying about 7200 cm^{-1} above the $1B_u$ state,[8] and in ATR, it is calculated to lie 6600 cm^{-1} above the $1B_u$ state.[8] Recent transient absorption experiments[56] also hint at a strong transition from the $1B_u$ state to a higher lying state. The presence of the heteroatom lowers the energy gap between the two states and may also serve to strengthen the transition dipole between them, increasing the "*m*Ag" contribution to the polarizability of the $1B_u$ state. The heteroatom also necessitates a dipole moment in the "*m*Ag" state, which is not present in the molecules studied thus far. Therefore, solvation of the polar retinal may further decrease the energy gap and/or increase the transition moment between the "*m*Ag" and $1B_u$ states.

Now we shall investigate the possibility that the large experimental $\overline{\Delta\alpha}$ value in alll molecules studied (compared to our calculations) is due to neglect of the terms containing the transition polarizability (see eq 2) during data analysis. The fact that our a_χ values were very small (2−3 orders of magnitude smaller than b_χ) and negative (Table 1) indicates that the second term (containing the transition hyperpolarizability) dominates or cancels the first (transition polarizability) term in eq 1. Symmetry arguments can be used to predict that the transition hyperpolarizability will dominate,[42] and this term plays no role in the calculation of $\overline{\Delta\alpha}$ from b_χ (see eq 2). However, the retinals do not strictly follow the symmetry rules, so the contribution may become significant. This large discrepancy could be reconciled by including the hyperpolarizability ($\underline{A}$) term in the $\overline{\Delta\alpha}$ calculation as described below.

Using the finite-field formalism, we were able to calculate the transition polarizability ($\underline{A}$) in ATR by expanding the transition dipole moment in the applied field. Although we realize that this number is only approximate, it allows us to estimate how large $\underline{A}$ can become in these polar molecules. Indeed, after calculating $\underline{A}$ we used it to calculate the first term in eq 2 ($(1/15|\underline{\mathbf{m}}|^2)\sum_{i,j}\mathbf{m}_i\underline{A}_{ij}\Delta\mu_j$) to obtain a value of about 24 Å^3 for the contribution to the polarizability (gas phase) and about 68 Å^3 in 13-CR. In the SB forms, this term contributes about 23 Å^3 to the polarizability in ATR-SB and up to 40 Å^3 in 13-CR-SB. These values are smaller than in the aldehydes, but are still significant contributions to $\overline{\Delta\alpha}$. We are not aware of how solvation would affect this term, but it is likely to increase. Because this term depends strongly on $\Delta\mu$, it becomes a significant factor only in molecules where $\Delta\mu$ is relatively large; thus it is negligible in the diphenylpolyenes.

Both the neglect of certain states in the α_e calculation and the neglect of the transition polarizability term during data analysis appear to be important in explaining the discrepancy between $\overline{\Delta\alpha_{calc}}$ and $\overline{\Delta\alpha}$ in the aldehydes. We note that large condensed-phase $\overline{\Delta\alpha}$ values are a general feature of many donor−acceptor polyenes that have appeared recently in the literature.[41,42] The possibility of molecular orientation effects in these systems can also not be ruled out at this time. Looking at eq 2, one can see that if the retinal was free to rotate even slightly, the contributions of the Boltzmann terms in this equation can become significant, especially in the case of retinals or other molecules where both μ_g and $|\Delta\underline{\mu}|$ are large.[57] The role of solute and/or solvent rotation on analysis of the Stark effect spectrum will be discussed in greater detail in another contribution.

Conclusions

In general, the INDO1S/SCI/FF method correctly predicts ground-state dipole moments and polarizabilities in both the aldehyde and SB forms of retinal, as well as the $\Delta\mu$ values in retinal aldehydes. However, we see large deviations in the calculated and measured values of $\Delta\mu$ in the SB forms of the retinals. We attribute this to isomer-dependent mixing of the B_u state with a second state (probably the $2A_g$ state) with a larger dipole moment. We also observe large deviations between experimental and calculated values of $\overline{\Delta\alpha}$, which suggest that additional factors, such as molecular orientation or transition polarizability effects, should be carefully considered when analyzing the Stark effect spectrum. In addition, calculations of excited-state polarizabilities in polar substituted polyenes may require the inclusion of higher lying or "forbidden" states that are stabilized in the condensed phase. We are currently investigating the excited-state polarizability calculation in more detail and will address these concerns in another contribution.

Acknowledgment. We would like to thank Dr. David Yaron for help with the polarizability calculation development and interpretation, Dr. Hyung Kim for useful discussions about solvation corrections, Dr. Zhigang Shuai and Professor J. L. Brédas for preliminary INDO/SCI/SOS calculations on ATR and substituted polyenes, Robert Bussell for electroabsorption measurements on ATR and work on our data analysis routines, and M. Charisse Davis, who was supported by a Howard Hughes Medical Institute grant, for preliminary work on the semi-empirical calculations. We would also like to thank our sources of funding: The Winters Foundation, the Petroleum Research Fund administered by the American Chemical Society, and the NSF-RPG and CAREER programs.

References and Notes

(1) Wald, G. *Nature* **1968**, *219*, 800−807.

(2) Oesterhelt, D.; Stoeckenius, W. *Nature, New Biol.* **1974**, *233*, 149−152.

(3) Birge, R. R. *Biochim. Biophys. Acta* **1990**, *1016*, 293−327.

(4) Ames, J. B.; Bolton, S. R.; Netto, M. M.; Mathies, R. A. *J. Am. Chem. Soc.* **1990**, *112*, 9007−9009.

(5) Ames, J. B.; Ros, M.; Raap, J.; Lugtenburg, J.; Mathies, R. A. *Biochemistry* **1992**, *31*, 5328−5334.

(6) Hendrickx, E.; Clays, K.; Persoons, A.; Dehu, C.; Brédas, J. L. *J. Am. Chem. Soc.* **1995**, *117*, 3547−3555.

(7) Birge, R. R.; Bocian, D. F.; Hubbard, L. M. *J. Am. Chem. Soc.* **1982**, *104*, 1196−1207.

(8) Hubbard, L. M. Ph.D. Thesis, Univ. of CA, Riverside, 1980.

(9) Merchan, M.; Gonzalez-Luque, R. *J. Chem. Phys.* **1997**, *106*, 1112−1122.

(10) Toto, J. L.; Toto, T. T.; de Melo, C. P.; Robins, K. A. *J. Chem. Phys.* **1994**, *101*, 3945−3951.

(11) de Melo Sales, T. R.; de Melo, C. P. *Chem. Phys. Lett.* **1991**, *180*, 105−108.

(12) Birge, R. R.; Bennett, J. A.; Hubbard, L. M.; Fang, H. L.; Pierce, B. M.; Kliger, D. S.; Leroi, G. E. *J. Am. Chem. Soc.* **1982**, *104*, 2519−2525.

(13) Murray, L. P.; Birge, R. R. *Can. J. Chem.* **1985**, *63*, 1967−1971.

(14) Hudson, B. S.; Kohler, B. E. *J. Chem. Phys.* **1973**, *59*, 4984−5001.

(15) Leopold, D. G.; Pendley, R. D.; Roebber, J. L.; Hemley, R. J.; Vaida, V. *J. Chem. Phys.* **1984**, *81*, 4218−4229.

(16) Buma, W. J.; Kohler, B. E.; Song, K. *J. Chem. Phys.* **1990**, *92*, 4622−4623.

(17) Sakurai, M.; Ando, I.; Inoue, Y.; Chujo, R. *Photochem. Photobiol.* **1981**, *34*, 367−374.

(18) Becker, R. S.; Hug, G.; Das, P. K.; Schaffer, A. M.; Takemura, T.; Yamamoto, N.; Waddell, W. *J. Phys. Chem.* **1976**, *80*, 2265−2273.

(19) Becker, R. S.; Freedman, K. *J. Am. Chem. Soc.* **1985**, *107*, 1477−1485.

(20) Freedman, K. A.; Becker, R. S. *J. Am. Chem. Soc.* **1986**, *108*, 1245−1251.

(21) Honig, B.; Greenberg, A. D.; Dinur, U.; Ebrey, T. G. *Biochemistry* **1976**, *15*, 4593−4599.

(22) Liptay, W. In *Modern Quantum Chemistry Part III: Action of Light and Organic Crystals*; Sinanoglu, O., Ed.; Academic Press: New York, 1965; pp 45−66.

(23) Bevington, P. R.; Robinson, D. K. *Data Reduction and Error Analysis for the Physical Sciences*, 2nd ed.; McGraw-Hill, Inc.: New York, 1992; p 328.

(24) In response to reviewers' concerns about purity of the samples, we did two experiments. First, electroabsorption measurements on 90% and >98% pure (recrystalized) ATR gave results that were within the error bars of one another. Second, we simulated contaminated spectra by adding increasing percentages of 9-CR data to an ATR spectrum. This experiment revealed that the purity of ATR would have to drop to below 70% to see a significant difference between $|\Delta\underline{\mu}|$ and $|\underline{\mathbf{m}}\cdot\Delta\underline{\mu}|$, and below 80% to see a significant change in $\overline{\Delta\alpha}$ or $\Delta\underline{\alpha}_m$.

(25) Irving, C. S.; Leermakers, P. A. *Photochem. Photobiol.* **1968**, *7*, 665−670.

(26) Liptay, W. In *Excited States*; Lim, E. C., Ed.; Academic Press: New York, 1974; pp 129−229.

(27) Ponder, M.; Mathies, R. *J. Phys. Chem.* **1983**, *87*, 5090−5098. In PMMA films (without the internal field factor), they measured $|\Delta\underline{\mu}| = 14.7 \pm 0.6$ D, $|\underline{\mathbf{m}}\cdot\Delta\underline{\mu}| = 15.6 \pm 2.0$ D, $\overline{\Delta\alpha} = 222 \pm 20$ Å^3, and $\Delta\underline{\alpha}_m = 738 \pm 100$ Å^3 for ATR.

(28) Mathies, R.; Stryer, L. *Proc. Natl. Acad. Sci. U.S.A.* **1976**, *73*, 2169-2173. In dioxane solutions, they measured $|\Delta\underline{\mu}| = 15.6 \pm 1.0$ D and $|\underline{\mathbf{m}}\cdot\Delta\underline{\mu}| = 14.7 \pm 2.1$ D for ATR, and $|\Delta\underline{\mu}| = 9.9 \pm 0.5$ D and $|\underline{\mathbf{m}}\cdot\Delta\underline{\mu}| = 10.2 \pm 0.9$ D for ATR-SB.

(29) Davidsson, A.; Johansson, L. B. *J. Phys. Chem.* **1984**, *88*, 1094−1098. In polyethylene (PE) and polypropylene (PP) films they measured $|\Delta\underline{\mu}| = 15.5 \pm 1.0$ D and $|\underline{\mathbf{m}}\cdot\Delta\underline{\mu}| = 15.6 \pm 1.5$ D, $\overline{\Delta\alpha} = 1000 \pm 300$ Å^3 in PE, and $\overline{\Delta\alpha} = 1500 \pm 630$ Å^3 in PE for ATR. These polarizability values should be regarded as an upper limit.

(30) Noggle, J. H. *Practical Curve Fitting and Data Analysis: Software and Self-Instruction for Scientists and Engineers*; PTR Prentice Hall: Englewood Cliffs, NJ, 1993; p 192.

(31) Dewar, M. J. S.; Zoebisch, E. G.; Healy, E. F.; Stewart, J. J. P. *J. Am. Chem. Soc.* **1985**, *107*, 3902−3909.

(32) Dewar, M. J. S.; Thiel, W. *J. Am. Chem. Soc.* **1977**, *99*, 4907−4917.

(33) Dewar, M. J. S.; Thiel, W. *J. Am. Chem. Soc.* **1977**, *99*, 4899−4906.

(34) Stewart, J. J. P. *J. Comput. Chem.* **1989**, *10*, 209−220.

(35) Kurtz, H. A.; Stewart, J. J. P.; Dieter, K. M. *J. Comput. Chem.* **1990**, *11*, 82−87.

(36) Kurtz, H. A. *Int. J. Quantum Chem.: Quantum Chem. Symp.* **1990**, *24*, 791−798.

(37) Ridley, J. E.; Zerner, M. C. *Theor. Chim. Acta (Berlin)* **1976**, *42*, 223−236.

(38) Ridley, J.; Zerner, M. *Theor. Chim. Acta (Berlin)* **1973**, *32*, 111−134.

(39) Bottcher, C. J. F. *Theory of Electric Polarisation*; Elsevier Publishing Co.: Amsterdam, 1952; p 492.

(40) *Handbook of Plastics*, 2nd ed.; Simonds, Weith, Bigelow, Eds.; D. Van Nostrand Co., Inc.: New York, 1949.

(41) Bublitz, G. U.; Ortiz, R.; Runser, C.; Fort, A.; Barzoukas, M.; Marder, S. R.; Boxer, S. G. *J. Am. Chem. Soc.* **1997**, *119*, 2311−2312.

(42) Bublitz, G. U.; Ortiz, R.; Marder, S. R.; Boxer, S. G. *J. Am. Chem. Soc.* **1997**, *119*, 3365−3376.

(43) For ATR (Table 1), our $|\Delta\underline{\mu}|$ are 30% to 40% lower and our $\overline{\Delta\alpha}$ are within the range of values previously reported by other groups utilizing electroabsorption (see refs 27−29). However, using a combination of dielectric constant data and solvatochromic behavior, Corsetti and Kohler (ref 60) estimated $|\Delta\underline{\mu}|$ to be 5.7 D, which is smaller than our measured value. In the retinal SB isomers (Table 2), $|\Delta\underline{\mu}|$ are larger than those of the aldehydes (Table 1) in both cis isomers and are within 30% of reported values (ref 28) for ATR-SB ($|\Delta\underline{\mu}| = 9.9$ D, $|\underline{\mathbf{m}}\cdot\Delta\underline{\mu}| = 10.2$ D).

(44) Simmons, C. J.; Liu, R. S. H.; Denny, M.; Seff, K. *Acta Crystallogr.* **1981**, *B37*, 2197−2205.

(45) Simmons, C. J. *Acta Crystallogr.* **1986**, *C42*, 1558−1563.

(46) Hamanaka, T.; Mitsui, T.; Ashida, T.; Kakudo, M. *Acta Crystallogr.* **1972**, *B28*, 214−222.

(47) Tallent, J. R.; Birge, J. R.; Zhang, C.-F.; Wenderholm, E.; Birge, R. R. *Photochem. Photobiol.* **1992**, *56*, 935−952.

(48) Another possibility exists, that the solvation correction is inadequate for $\Delta\alpha$ in polar molecules. Note that in eq 5 there are no terms that depend on μ_g. One might expect that a term of this type would be necessary to adequately model solvent effects on $\Delta\alpha$ in polar systems. We are currently investigating calculations of this type.

(49) Luzhkov, V.; Warshel, A. *J. Am. Chem. Soc.* **1991**, *113*, 4491−4499.

(50) Jonsson, D.; Norman, P.; Luo, Y.; Agren, H. *J. Chem. Phys.* **1996**, *105*, 581−587.

(51) Hasegawa, T.; Ishikawa, K.; Kanetake, T.; Koda, T.; Takeda, K.; Kobayashi, H.; Kubodera, K. *Chem. Phys. Lett.* **1990**, *171*, 239−244.

(52) Chance, R. R.; Shand, M. L.; Hogg, C.; Silbey, R. *Phys. Rev. B* **1980**, *22*, 3540−3550.

(53) van Beek, J. B.; Albrecht, A. C. *Chem. Phys. Lett.* **1991**, *187*, 269−276.

(54) van Beek, J. B.; Kajzar, F.; Albrecht, A. C. *J. Chem. Phys.* **1991**, *95*, 6400−6412.

(55) Dixit, S. N.; Guo, D.; Mazumdar, S. *Phys. Rev. B* **1991**, *43*, 6781−6784.

(56) Larson, E. J.; Friesen, L. A.; Johnson, C. K. *Chem. Phys. Lett.* **1997**, *265*, 161−168.

(57) Assuming all of the measured $\overline{\Delta\alpha}$ arises from orientation (nuclear) polarization allows us to estimate the extent of ATR reorientation to be ±10−20°. This amounts to a total of 20−40°, which is very large considering the size of the retinal. It is also possible that solvent molecules trapped in the polymer matrix may be reorienting.

(58) Schaffer, A. M.; Waddell, W. H.; Becker, R. S. *J. Am. Chem. Soc.* **1974**, *96*, 2063−2068.

(59) Liptay, W.; Wortmann, R.; Bohm, R.; Detzer, N. *Chem. Phys.* **1988**, *120*, 439−448.

(60) Corsetti, J. P.; Kohler, B. E. *J. Chem. Phys.* **1977**, *67*, 5237−5243.